

1
2
3
4 Article type : Technical Paper
5
6

7 **Assessment of the Extreme Rainfall Event at Nashville, Tennessee and the Surrounding**
8 **Region on May 1-3, 2010**
9

10 Barry D. Keim, William D. Kappel, Geoffrey A. Muhlestein, Douglas M. Hultstrand, Tye W.
11 Parzybok, Amanda B. Lewis, Edward M. Tomlinson, and Alan W. Black
12

13 Department of Geography & Anthropology (**Keim, Black**), Louisiana State University, Baton Rouge,
14 Louisiana, USA; Applied Weather Associates (**Kappel, Muhlestein, Hultstrand**), Monument, Colorado,
15 USA; METSTAT Inc. (**Parzybok**), Fort Collins, Colorado, USA; Engineering Research and
16 Development Center (**Lewis**), U.S. Army Corps of Engineers, Vicksburg, Mississippi, USA; and
17 Atmospheric Science Consultants (**Tomlinson**), Colorado Springs, Colorado, USA (Correspondence to
18 Keim: keim@lsu.edu).
19

20 **Research Impact Statement:** The maximum rainfall totals for some durations during the May
21 1–3, 2010 storm event at Nashville, TN exceeded the 1000-yr rainfall values from NOAA Atlas
22 14 warranting a reevaluation of design storms.
23

24 **ABSTRACT:** This paper analyzes the May 1–3 2010 rainfall event that affected the south-
25 central United States, including parts of Mississippi, Tennessee, and Kentucky. The storm is
26 evaluated in terms of its synoptic setting, along with the temporal distributions, and spatial
27 patterns of the rainfall. In addition, the recurrence interval of the storm is assessed and the
28 implications for hydrologic structure designs are discussed. The event was associated with an
29 upper-level trough and stationary frontal boundary to the west of the rainfall region, which
30 remained quasi-stationary for a period of 48 hours. Heavy rainfall was produced by two slow-
**This is the author manuscript accepted for publication and has undergone full peer review but has
not been through the copyediting, typesetting, pagination and proofreading process, which may
lead to differences between this version and the Version of Record. Please cite this article as doi:
[10.1111/1752-1688.12657-17-0076](https://doi.org/10.1111/1752-1688.12657-17-0076)**

31 moving mesoscale convective complexes (MCC), combined with abundant atmospheric
32 moisture. Storm totals exceeding 330 mm occurred within a large elongated area extending from
33 Memphis to Nashville. Isolated rainfall totals over 480 mm were reported in some areas, with
34 NEXRAD weather radar rainfall estimates up to 501 mm. An extreme value analysis was
35 performed for 1- and 2- day rainfall totals at Nashville and Brownsville, Tennessee, as well as
36 for gridded rainfall estimates for the entire region using the Storm Precipitation Analysis System
37 (SPAS). Results suggest maximum rainfall totals for some durations during the May 1–3, 2010
38 event exceeded the 1,000-yr rainfall values from NOAA Atlas 14 for a large portion of the
39 region and reached up to 80 percent of the Probable Maximum Precipitation (PMP) values for
40 some area sizes and durations.

41
42 **(KEYWORDS:** flooding; meteorology; precipitation; statistics.)

44 INTRODUCTION

45 On May 1–3, 2010, record-breaking rainfall dramatically affected the region surrounding
46 Nashville, Tennessee. These rains led to severe flash flooding in the city and river basin
47 flooding, particularly on the Cumberland River. The flooding caused 26 deaths in Tennessee and
48 Kentucky, but the hardest hit area was Nashville (National Weather Service, 2011). The storm
49 broke previous record rainfall totals for a large portion of the south-central U.S. Prior to this
50 event, the most extreme rainfall records in this region were associated with tropical cyclones,
51 such as Hurricane Frederic in 1979 and Hurricane Katrina in 2005 (Durkee et al., 2012). This
52 storm stands out, not only because it exceeded previous rainfall records by substantial margins,
53 but also because it was initiated by a mid-latitude cyclone that interacted with extremely high
54 atmospheric moisture levels. A number of studies have examined various aspects of this
55 significant and impactful storm. The storm’s physical mechanisms were explored by two studies
56 (Moore et al., 2012; 2015), while others investigated the synoptic environment (Durkee et al.,
57 2012), forecasting difficulties (Lynch and Schumacher, 2014), and potential enhancement due to
58 climate change (Lackmann, 2013). However, a detailed analysis of the rareness of this storm and
59 its implications for hydrological planning and risk management in the hardest hit areas has not
60 been completed.

61 The May 2010 flood event that resulted from these record rains established the new flood
62 of record for most of the Cumberland River (U.S. Army Corps of Engineers, 2010). The
63 flooding nearly overwhelmed the locks and dams along the river. At Cordell Hull Dam near
64 Carthage, TN, water was within 0.05m of overtopping the lock gates (U.S. Army Corps of
65 Engineers, 2010). A similar situation occurred at Old Hickory Dam immediately upstream of
66 Nashville, where water was within 0.16m of overtopping the lock wall (U.S. Army Corps of
67 Engineers, 2010). Given the vicinity of Old Hickory to Nashville, overtopping of the lock gates
68 would have resulted in a crest approximately 1.22m higher in Nashville itself (U.S. Army Corps
69 of Engineers, 2010). Therefore, it is important to consider this storm event for future
70 infrastructure development in the region, especially hydrologic structure designs. Given the
71 extreme nature of the storm and its impacts, this paper 1) summarizes the meteorological
72 conditions associated with the storm, 2) describes the spatial pattern and temporal distribution of
73 the rainfall, 3) discusses the implications for probable maximum precipitation (PMP) studies, and
74 4) assesses this storm's recurrence interval using extreme value statistics.

75 This study adds to a growing list of case study papers on heavy rainfall, including
76 Caracena and Fritsch (1983) on the Texas Hill Country Flash Floods of 1978, Leathers et al.
77 (1998) on the rain on snow floods of January 1996 in North-Central Pennsylvania, Keim (1998)
78 on the record rainfalls during the coastal storm in Maine in October 1996, Changnon and Kunkel
79 (1999) who examined the rainstorms and flooding of July 1996 in Chicago, and Wang et al.
80 (2016) who performed an attribution study of the Louisiana flood of August 2016, among many
81 others. This storm is also one of several impressive rainfall events that have occurred across the
82 Eastern United States over the past 8-10 years, including in South Carolina (October 2-4, 2015),
83 West Virginia (June 23-24, 2016), Ellicott City, Maryland (July 30, 2016), and Hurricane
84 Harvey's rains in southeastern Texas (August 25-31) (See the list of reports from the
85 Hydrometeorological Design Studies Center
86 at http://www.nws.noaa.gov/oh/hdsc/aep_storm_analysis/). Collectively, this assemblage of
87 recent heavy rainfall events does raise the question whether global climate change is having an
88 impact on the heavy rainfall climatology of the region. Two recent papers did note that climate
89 change enhanced the probability for such events to occur, e.g., in Louisiana in August 2016 (van der Wiel
90 et al. 2017) and during Hurricane Harvey in Texas (van Oldenborgh et al. 2017).

91 METEOROLOGICAL SETTING OF STORM

92 At 1200 UTC on May 1, 2010, the entire eastern half of the United States was in some
93 way under the influence of an occluded mid-latitude cyclone with its associated surface low
94 pressure center anchored over North Dakota, Minnesota and southern Manitoba, Canada (Figure
95 1). A warm front extended across the Great Lakes into southern New England, with an
96 associated cold/stationary front extending over the Mississippi River Valley. Precipitation was
97 ongoing across western Tennessee and Kentucky. At this time, the Nashville region and much of
98 the southeastern United States was within the warm sector of the storm system.

99 The next set of images at 1200 UTC on May 2 shows that the center of low pressure
100 migrated slowly southeastward, and the trailing cold front only advanced eastward modestly. The
101 slow movement of the surface front was associated with the stagnant 500 mb pattern
102 characterized by winds parallel to the frontal boundary. Rainfall was enhanced by the
103 propagation of a series of 500 mb shortwave troughs that moved over the Nashville region on
104 May 1 and 2 and initiated a pair of slow-moving Mesoscale Convective Complexes (MCCs).
105 Most of the rain fell during these two calendar days. By May 3, the cold front had moved
106 eastward past Nashville, ending the rainfall over the Nashville region. Little rainfall was
107 produced by the secondary cold front that followed closely behind.

108 While the overall synoptic setting of the storm was not particularly unusual, the quasi-
109 stationary nature of the storm, combined with very high precipitable water levels that originated
110 over the Caribbean and Gulf (Higgins et al., 2011; Lynch and Schumacher, 2014), were unusual.
111 An extremely moist atmospheric airmass was in place that originated from the Caribbean and
112 Gulf of Mexico, as shown in Figure 2 by the HYSPLIT atmospheric trajectory model (Draxler
113 and Rolph, 2014; Rolph, 2014). This model can be used to determine the source region of an air
114 particle using a backward trajectory over a period of days, which in this case is stepped back in
115 time over 72 hours. This flow regime from the Caribbean, termed the Maya Express by Dirmeyer
116 and Kinter (2009), is one of several types of “atmospheric rivers” (Mahoney et al. 2016) that are
117 responsible for rapid moisture transport from tropical regions to the mid-latitudes. The highest
118 precipitable water values ever observed in 60 years of records were measured at both Jackson,
119 Mississippi and Nashville, Tennessee on May 1–3 2010. This rare combination of events allowed
120 the historic flooding event to unfold. For a more detailed synoptic analysis of the storm, refer to
121 Durkee et al. (2012).

122 **SPATIAL AND TEMPORAL PATTERNS OF RAINFALL**

123 The primary hydro-meteorological rainfall analysis tool used in this study is the Storm
124 Precipitation Analysis System, or SPAS (Parzybok and Tomlinson, 2006). SPAS is a gridded
125 rainfall analysis software package that combines all available rainfall data, including rain gauge
126 data (daily, hourly and sub-hourly), supplemental/bucket survey rainfall data, dynamically
127 calibrated NEXRAD weather radar data, and climatological basemaps, to produce a high
128 resolution, spatially continuous gridded analysis of rainfall amounts. Rainfall values are
129 produced at time intervals as short as 5-minutes, and at spatial scales as fine as 1 km² (Parzybok
130 and Tomlinson, 2006). The system is designed to reproduce the spatio-temporal pattern of a
131 rainfall event across a region. It provides highly accurate estimates of rainfall values between
132 rainfall observation locations, thereby allowing for an accurate representation of accumulated
133 rainfall in both space and time across the rainfall domain. In our database of storms across the
134 United States, the Nashville storm is No. 1208, which appears in several of the figures used in
135 this paper. Additional detail on the SPAS system are found in Parzybok and Tomlinson (2006).

136 While rainfall totals exceeding 125 mm were observed from northern Mississippi to
137 central Kentucky, the heaviest rainfall produced by this storm system was concentrated in an
138 elongated band extending from Memphis to Nashville (Figure 3). The analyzed rainfall fell from
139 May 1 at 0100 UTC to 3 May at 1200 UTC. Storm totals exceeded 330 mm for most of the area
140 in this band. Even higher precipitation totals were nested within the band, including storm totals
141 of over 480 mm at multiple locations. The SPAS analysis produced a storm maximum rainfall
142 total of 501 mm at 36.06° N and 86.91° W, or about 6 kilometers north-northeast of Camden,
143 Tennessee. This location is the storm center for this event.

144 An hourly time-series of rainfall from May 1 at 0100 UTC to May 3 at 1200 UTC at the
145 storm center shows several intense short-duration rainfall periods, imbedded within two longer
146 periods of heavy rainfall (Figure 4). The timing of the two waves of heavy rainfall corresponds
147 to the passage of two upper-level shortwaves and associated MCCs. The first wave of rain began
148 on May 1 at 1100 UTC and ended about 0100 UTC on May 2, with two hourly accumulations
149 that exceeded 25 mm. The first wave produced over 250 mm of rain. The second wave of rain on
150 May 2 began after 1200 UTC and ended around 2300 UTC, with three hourly accumulations that
151 exceeded 25 mm. The second wave produced an additional 200 mm of rain.

152 **HYDROLOGIC DESIGN APPLICATION**

153 To quantify the magnitude and extent of the rainfall, a Depth-Area–Duration (DAD) table
154 was generated for the storm event using SPAS. The maximum average depth of precipitation at
155 various time durations was computed for area sizes up to 129,500 km² (50,000 mi²) surrounding
156 the storm center (Table 1). The non-traditional area sizes in km² are used here to maintain
157 continuity with other hydrometeorological publications used in the United States (i.e., Schreiner
158 and Riedel (1978) and U.S. Army Corps of Engineers (1973) storm studies). This type of
159 analysis is very important for assessing hydrological impacts, because it provides the volume of
160 rainfall that fell over various area sizes during the storm. This analysis shows that an average of
161 197 mm of rain fell across a region of 129,500 km² (50,000 mi²) over a 60 hour period – an area
162 larger than the entire state of Tennessee. In addition, 416 mm of rainfall fell over an area of
163 5,180 km² (2,000 mi²) over the same duration, and 118 mm was the absolute 1-hour rainfall
164 maximum, which fell at latitude 35.61 N and 89.26 W, near Brownsville in western Tennessee.
165 The impressive amount of rain that fell over such a large area compounded by the extreme
166 rainfall intensity over short time durations help to explain why this event caused such
167 catastrophic flooding throughout the region.

168 To further demonstrate how impressive these rainfall totals are for the region, they are
169 compared to Probable Maximum Precipitation (PMP) estimates from *Hydrometeorological*
170 *Report No. 51* (Schreiner and Riedel, 1978) for varying durations and area sizes. PMP as defined
171 by Corrigan et al. (1999, p. 5) is "theoretically, the greatest depth of precipitation for a given
172 duration that is physically possible over a given storm area at a particular geographical location
173 at a certain time of the year." As such, rainfall values even approaching PMP estimates would
174 suggest a very rare storm. The 48-hour/25,900 km² (10,000 mi²) and the 48-hour/51,800
175 km² (20,000 mi²) rainfall values are found to be approximately 80 percent of the PMP values for
176 the region (Schreiner and Reidel, 1978). This gives testament to the unusual nature of this storm.
177 This has utility because PMP is one of the most important parameters used to develop design
178 criteria for dams and evaluate existing structures for dam safety.

179 In the determination of PMP values, not only are rare storms analyzed, but they are also
180 maximized to estimate how much more rainfall could have been produced if the maximum
181 amount of atmospheric moisture had been available to the storm at the time of its occurrence.
182 This process, called storm maximization, requires that the atmospheric moisture actually
183 associated with the storm system be quantified using surface dew point temperature observations

184 (World Meteorological Organization, 2009). This dew point temperature value is known as the
185 storm representative dew point (Schreiner and Riedel, 1978). To maximize the rainfall, a
186 climatological maximum dew point temperature is determined for the same location where the
187 storm representative dew point was observed. The 100-year return period maximum dew point
188 temperature is often used for the maximum dew point temperature value (e.g. Kappel et al. 2014;
189 Kappel et al. 2015a).

190 Using methods provided by the World Meteorological Organization (2009) PMP Manual,
191 the storm representative dew point temperature location for this storm was determined to be
192 31.50° N and 90.00° W, approximately 360 miles south-southwest of the storm center. It is
193 inappropriate to use dew point values within the area of rainfall production, as dew point
194 temperatures under these conditions do not always reflect the incoming airmass. This location
195 was determined to best represent the atmospheric environment that contributed to the event's
196 rainfall production. A parcel trajectory model (HYSPLIT; Draxler and Rolph, 2014) was used to
197 assist in identifying this location and timing ahead of the storm from which to select the dew
198 points (Figure 2). Surface dew point temperature observations surrounding the storm
199 representative dew point location were collected and the 12-hour average dew point temperature
200 value was determined by averaging observed dew point temperature values from the following
201 weather stations; Jackson, Mississippi (KJAN); McComb, Mississippi (KMCB); Hattiesburg,
202 Mississippi (KHBG); and Slidell, Louisiana (KASD). From these stations, the storm
203 representative dew point was determined to be 24.0°C.

204 To determine PMP values like those provided in *Hydrometeorological Report No. 51*
205 (Schreiner and Riedel, 1978), storms are “maximized” to increase the storm’s rainfall to its full
206 potential based on the largest possible dew point for the time of year in which the storm
207 occurred, plus or minus a window of time of 2 weeks from the occurrence date of the storm. In
208 this case, the 100-year 12-hour recurrence interval value for maximum dew point temperatures in
209 the southeastern United States from Tomlinson et al. (2013) was used to maximize this storm.
210 The 100-year 12-hour recurrence interval value was determined to be 25.0°C. Assuming a
211 saturated atmosphere, these dew point temperatures (storm representative dew point temperature
212 of 24.0°C and the 100-year return period dew point temperature of 25.0°C) correspond to
213 precipitable water values of 72 mm and 78 mm, respectively (U.S. Department of Commerce,
214 1951). Using procedures recommended by the World Meteorological Organization PMP Manual

215 (2009), these two values produce a maximization factor of 1.08 (78mm/72mm), which indicates
216 that in a worst-case scenario, this storm could have produced 8 percent more rainfall than it did,
217 assuming the maximum level of moisture was available to the storm for rainfall production and
218 the storm dynamics remained constant. In hydrologic design, these larger values (Table 1 values
219 multiplied by 1.08) would be used to represent this storm at the location of occurrence, and then
220 the storm could be transposed to other locations and modified according the World
221 Meteorological Organization (2009) guidelines. Factoring in maximization and transposition,
222 recent site-specific PMP analysis have shown that the inclusion of this storm impacts PMP
223 estimates for parts of the south central U.S. (Tomlinson et al., 2013; Kappel et al., 2014; Kappel
224 et al., 2015a; Kappel et al., 2015b).

225 **RECURRENCE INTERVALS**

226 Recurrence intervals are often calculated for an event for a variety of different time
227 durations, typically ranging from hours to days (i.e., see Keim, 1998). This often leads to
228 confusion, because the recurrence interval values vary depending on the duration that is being
229 examined. For example, the 100-yr return period calculated for a 24-hour duration is not the
230 same as the 100-year return period calculated for a one-day duration (Hershfield, 1961). Return
231 periods calculated for 24-hour durations are determined from the greatest 24-hour rainfall that
232 occurred during an event, which is derived from hourly rainfall observations that are passed
233 through a moving window and can span calendar days. However, the number of sites that record
234 hourly rainfall observations is limited. Therefore, it is common to calculate return periods for
235 observational day durations, which are collected at a larger number of sites and therefore provide
236 improved spatial coverage of an event. However, using observational day data limits the amount
237 of temporal analysis that can be applied to the data. Conveniently, SPAS provides hourly rainfall
238 values for each grid cell for the duration of the event, allowing for both a thorough temporal
239 analysis and a complete spatial analysis of the storm's recurrence intervals. In this analysis, both
240 SPAS data combined with regional data from *NOAA Atlas 14* (NA14) Volume 2 (Bonnin et al.,
241 2006) are used in one analysis and individual station data are analyzed in another.

242 With both datasets, an extreme value analysis was performed for the entire region using
243 quantile estimating methods identical to those used in the current Precipitation Frequency Atlas
244 of the United States, (NA14) Volume 2. The quantile estimates in NA14 were determined using
245 annual maximum series (AMS) rainfall data, which are converted to represent partial duration

246 series (PDS) data. AMS data were used in conjunction with L-moment analysis and the
247 generalized extreme value (GEV) distribution (Hosking, 1990; Stedinger et al., 1993; Hosking
248 and Wallis, 1997). L-moments are defined as expectations of certain linear combinations of
249 order statistics (Hosking, 1990). They are analogous to conventional moments with measures of
250 location (mean), scale (standard deviation), and shape (skewness and kurtosis). The GEV
251 distribution is a mathematical form that incorporates Gumbel's type I, II, and III distributions for
252 maxima (Stedinger et al., 1993). The parameters of the GEV distribution are the ξ (location
253 parameter), α (scale parameter) and k (shape parameter). The Gumbel, type I, is obtained when
254 $k = 0$. For $k > 0$, the distribution has finite upper bound at $\xi + \alpha / k$ and corresponds to the type
255 III distribution for maxima that is bounded from above (Stedinger et al., 1993). Stations with
256 records of sufficient length (30 years for daily stations and 20 years for hourly stations)
257 extending up to December 2000 were used in NA14 (Bonnin et al., 2006) and this criterion was
258 used here. The stations were grouped into small regions and the appropriate distribution function
259 among the GEV family of distributions was determined for each region using goodness-of-fit
260 tests. Once determined, the appropriate distribution was used to fit the AMS and generate
261 quantile estimates at each station, which are then adjusted to represent precipitation frequency
262 estimates via a PDS (Bonnin et al., 2006).

263 The quantile estimates were spatially interpolated to produce continuous quantile
264 estimates for the entire region. To determine the recurrence intervals for the extreme rainfall
265 event in the Nashville region, quantile estimates for recurrence intervals of 2-years through
266 1,000-years were extracted from NA14 for the center of each SPAS grid cell for the 24-hour
267 period with the heaviest rainfall. The SPAS rainfall values were translated into average
268 recurrence intervals based on where they fell in the spectrum of recurrence interval estimates
269 from NA14. Results are presented in Figure 5. A significant area in central Tennessee and part
270 of northern Alabama has 24-hour maximum rainfall recurrence intervals of 1000-years or more,
271 surrounded by progressively larger areas exceeding the 500-year and 100-year recurrence
272 intervals.

273 To further put this rainfall event into perspective, the recurrence intervals for rainfall
274 totals at the stations of Nashville and Brownsville, Tennessee at 1- and 2-day durations were
275 determined, and compared with the recurrence intervals of previous heavy rainfall events at these
276 sites. Note that the Nashville and Brownsville analyses were an "at-site" statistical analysis,

277 whereas the SPAS data to NA14 comparison, previously discussed, provided spatially
278 continuous recurrence intervals based on a regional analysis. Nashville has a rainfall record of
279 74 years, while at Brownsville there are 109 years of data. Nashville was chosen because it is the
280 location of the historic flooding and Brownsville, Tennessee was chosen because it is located
281 near the area that received the maximum precipitation during the event. The recurrence intervals
282 for the top five largest events at each location for one-day and two-day durations are displayed in
283 Tables 2 and 3. Again, the recurrence interval estimates were determined based on the GEV
284 distribution, which was the best fit for both locations. For all four instances, the largest rainstorm
285 on record occurred during this 2010 event. In Nashville, the recurrence interval for the storm at
286 the one-day duration was nearly 800 years (Table 2). In addition, the first and third highest one-
287 day rainfall events occurred on May 2 and May 1, respectively. When calculated for the two-day
288 duration, the rainfall total is 345 mm, which is over twice the magnitude of the previous largest
289 2-day rainfall event Nashville produced by the remnant of Hurricane Frederick in September
290 1979. The recurrence interval for the storm at Nashville was determined to be almost a 14,000-
291 year event, and greatly exceeds the recurrence interval for any other two-day duration storm.
292 This recurrence interval is extrapolated well beyond the Nashville period of record and as a
293 result, this return interval must be interpreted judiciously; however, the rarity of this event does
294 punctuate just how large of an outlier this storm is relative to the other rainfall events at
295 Nashville. The one-day maximum rainfall event at Brownville is also produced by the May 2010
296 event at 406 mm (Table 3). This value is also over twice the value of the previous largest storm
297 on record. The recurrence interval at Brownsville is over 900 years for the 1-day duration. Due
298 to its location further west, the majority of the rain fell at Brownsville on May 1, 2010. The two-
299 day recurrence interval at Brownsville is over 1,000 years.

300 **SUMMARY AND CONCLUSIONS**

301 The heavy rainfall event of May 1–3 2010 was caused by the interaction of two upper-
302 level shortwave troughs with a stationary front and abundant atmospheric moisture that persisted
303 in the region for nearly 48 hours. This storm produced record amounts of rainfall and caused
304 catastrophic river flooding in Mississippi, Tennessee, and Kentucky. The highest rainfall totals
305 from the event occurred along a band from just north of Memphis to Nashville, and set one- and
306 two-day rainfall records throughout the region, exceeding previous records set by the remnant of
307 Hurricane Frederic in 1979 by over 100 percent. The maximum 24-hour rainfall totals during the

308 period of May 1–3 2010 exceeded the 1,000-year rainfall estimates in a large portion of the
309 region. Rainfall values for the region for some durations and drainage area sizes came within 80
310 percent of NOAA PMP estimates (Schreiner and Reidel, 1978) and are controlling (sets the upper
311 limit) of updated PMP values in several recent site-specific and region PMP studies (e.g. Kappel
312 et al., 2014). After factoring in maximization and transposition of this storm, our data show that
313 recent site-specific PMP analyses would indeed be impacted in other parts of the south-central
314 U.S. by this storm. This storm was a remarkably efficient rain producer; PMP maximization
315 found that this storm in a worst-case scenario would have only produced 8% more precipitation
316 than the event that actually occurred. While this efficiency is impressive, it is important to
317 recognize that greater rainfall totals are theoretically possible in the region and to account for
318 that possibility in future hydrological planning and risk management.

319 There is clearly need to continue to analyze both old and new storms to further
320 understand and refine our understanding of PMP across the United States and beyond. The
321 implications are that dam design across the United States is either over or under engineered. The
322 only way to make this determination is through PMP analysis, which is frequently conducted on
323 a site-specific basis - in other words for only a single watershed and dam at a time. As such,
324 results (varying rainfall amounts over varying area sizes for durations from 1 to 60 hours) from
325 this storm can be used as candidate values in PMP analysis, along with similar information from
326 other storms. With that in mind, the methods used in this paper also provide a framework for
327 analysis of other storms of varying shapes and sizes relevant in the world of PMP – down to
328 sizes of less than 1km² to well over 50km². However, we note that these analyses are only as
329 robust as the data quantity and quality available. Furthermore, Kunkel (2013)) and van der Wiel
330 et al. (2016) suggest that impacts of climate change also be considered in such analyses.

331 ACKNOWLEDGMENTS

332 This paper was supported by NOAA Grants NA080AR4320886 and NA13OAR4310183.
333 Original datasets are from the National Oceanographic and Atmospheric Administration.

334 LITERATURE CITED

335 Bonnin, G., D. Martin, B. Lin, T. Parzybok, M. Yekta, and D. Riley, 2006. *NOAA Atlas 14*
336 *Volume 2, Precipitation-Frequency Atlas of the United States*, Delaware, District of
337 Columbia, Illinois, Indiana, Kentucky, Maryland, New Jersey, North Carolina, Ohio,

338 Pennsylvania, South Carolina, Tennessee, Virginia, West Virginia. NOAA, National Weather
339 Service, Silver Spring, Maryland.

340 Caracena, F., and J.M. Fritsch, 1983. Focusing Mechanisms in the Texas Hill Country Flash
341 Floods of 1978. *Monthly Weather Review* 111:2319-2332. DOI: 10.1175/1520-
342 0493(1983)111<2319:FMITTH>2.0.CO;2

343 Changnon, S.A., and K.E. Kunkel, 1999. Record Flood-Producing Rainstorms of 17-18 July
344 1996 in the Chicago Metropolitan Area. Part 1: Synoptic and Mesoscale Features. *Journal of*
345 *Applied Meteorology* 38(3):257-265. DOI: 10.1175/1520-
346 0450(1999)038<0257:RFPROJ>2.0.CO;2

347 Corrigan, P., D.D. Fenn, D.R. Kluck, and J.L. Vogel, 1999. Probable maximum precipitation for
348 California. *Hydrometeorological Report No. 59*. U.S. Department of Commerce:
349 Washington D.C.

350 Dirmeyer, P.A., and J.L. Kinter, 2009. The “Maya Express”: Floods in the U.S. Midwest. *EOS*
351 *Transactions, American Geophysical Union* 90(12):101-103.
352 DOI.org/10.1029/2009EO120001

353 Draxler, R.R. and G.D. Rolph, 2014. HYSPLIT (HYbrid Single-Particle Lagrangian Integrated
354 Trajectory). NOAA Air Resources Laboratory, Silver Spring, Maryland.
355 <http://ready.arl.noaa.gov/HYSPLIT>.

356 Durkee, J. D., L. Campbell, K. Berry, D. Jordan, G. Goodrich, R. Mahmood and S. Foster, 2012.
357 A Synoptic Perspective of the Record 1-2 May 2010 Mid-South Heavy Precipitation Event.
358 *Bulletin of the American Meteorological Society* 93:611-620. DOI: 10.1175/BAMS-D-11-
359 00076.1

360 Hershfield, D.M., 1961. Rainfall Frequency Atlas of the United States. *Weather Bureau*
361 *Technical Paper No. 40*. U.S. Department of Commerce: Washington, D.C.

362 Higgins, R.W., V.E. Kousky, and P. Xie, 2011. Extreme Precipitation Events in the South-
363 Central United States during May and June 2010: Historical Perspective, Role of ENSO, and
364 Trends. *Journal of Hydrometeorology* 12:1056-170. DOI: 10.1175/JHM-D-10-05039.1

365 Hosking, J. R. M., 1990. L-moments: Analysis and estimation of distributions using linear
366 combinations of order statistics. *Journal of the Royal Statistical Society B* 52(1):105-124.

- 367 Hosking, J.R.M. and J.R. Wallis, 1997. *Regional Frequency Analysis: An Approach Based on L-*
368 *Moments*, Cambridge, UK Cambridge University Press, pp 240.
- 369 Kappel, W.D., D.M. Hultstrand, G.A. Muhlestein, K.M. Steinhilber, D.K. McGlone, T.W.
370 Parzybok, and E.M. Tomlinson, 2014. Statewide Probable Maximum Precipitation (PMP)
371 Study for Wyoming. <http://wwdc.state.wy.us/PMP/PMP.html>.
- 372 Kappel, W.D., D.M. Hultstrand, G.A. Muhlestein, K.M. Steinhilber, D.K. McGlone, T.W.
373 Parzybok, E.M. Tomlinson, and B. Lawrence, 2015a. Regional Probable Maximum
374 Precipitation (PMP) Study for the Tennessee Valley Authority (TVA).
- 375 Kappel, W.D., D.M. Hultstrand, G.A. Muhlestein, K.M. Steinhilber, D.K. McGlone, T.W.
376 Parzybok, E.M. Tomlinson, and B. Lawrence, 2015b. Statewide Probable Maximum
377 Precipitation (PMP) Study Virginia. [http://www.dcr.virginia.gov/dam-safety-and-](http://www.dcr.virginia.gov/dam-safety-and-floodplains/pmp-tool)
378 [floodplains/pmp-tool](http://www.dcr.virginia.gov/dam-safety-and-floodplains/pmp-tool).
- 379 Keim, B. D., 1998. Record Precipitation Totals from the Coastal New England Rainstorm of 20-
380 21 October 1996. *Bulletin of the American Meteorological Society* 79:1061-
381 1067. DOI: 10.1175/1520-0477(1998)079<1061:RPTFTC>2.0.CO;2
- 382 Kunkel, K.E., T.R. Karl, D.R. Easterling, K. Redmond, J. Young, X.G. Yin, P. Hennon, 2013.
383 Probable Maximum Precipitation and Climate Change. *Geophysical Research Letters*
384 40(7):1402-1408. DOI: 10.1002/grl.50334
- 385 Lackmann, G. M., 2013. The South-Central U.S. Flood of May 2010: Present and Future.
386 *Journal of Climate* 26:4688-4709. DOI: [10.1175/JCLI-D-12-00392.1](https://doi.org/10.1175/JCLI-D-12-00392.1)
- 387 Leathers, D.J., D.R. Kluck, and S. Kroczyński, 1998. The Severe Flooding Event of January
388 1996 across North-Central Pennsylvania. *Bulletin of the American Meteorological Society*
389 79(5):785-797. DOI: 10.1175/1520-0477(1998)079<0785:TSFEOJ>2.0.CO;2
- 390 Lynch, S.L., and R.S. Schumacher, 2014. Ensemble-based Analysis of the May 2010 Extreme
391 Rainfall in Tennessee and Kentucky. *Monthly Weather Review* 142(1):222-
392 239. DOI: 10.1175/MWR-D-13-00020.1
- 393 Mahoney, K. D.L. Jackson, P. Neiman, M. Hughes, L. Darby, G. Wick, A. White, E. Sukovich,
394 and R. Cifelli, 2016. Understanding the Role of Atmospheric Rivers in Heavy Precipitation

395 in the Southeast United States. *Monthly Weather Review* 144:1617-
396 1632. DOI: 10.1175/MWR-D-15-0279.1

397 Moore, B. J., P. J. Neiman, F. M. Ralph and F. E. Barthold, 2012. Physical Processes Associated
398 with Heavy Flooding Rainfall in Nashville, Tennessee, and Vicinity During 1-2 May 2010:
399 The Role of an Atmospheric River and Mesoscale Convective Systems. *Monthly Weather*
400 *Review* 140:358-378. DOI: 10.1175/MWR-D-11-00126.1

401 Moore, B.J., K.M. Mahoney, E.M. Sukovich, R. Cifelli, and T.M. Hamill, 2015. Climatology
402 and Environmental Characteristics of Extreme Precipitation Events in the Southeastern
403 United States. *Monthly Weather Review* 143:718-741. DOI: 10.1175/MWR-D-14-00065.1

404 National Weather Service, 2011. *Record Floods of the Greater Nashville: Including Flooding in*
405 *Middle Tennessee and Western Kentucky, May 1-4, 2010*. National Weather Service: Silver
406 Spring, Maryland, 67 pp. http://www.nws.noaa.gov/os/assessments/pdfs/Tenn_Flooding.pdf.

407 Parzybok, T.W., and E.M. Tomlinson, 2006. A New System for Analyzing Precipitation from
408 Storms. *Hydro Review* 25:58-65.

409 Rolph, G.D., 2014. Real-time environmental applications and display system (READY) Website
410 (<http://ready.arl.noaa.gov>). NOAA Air Resources Laboratory; Silver Spring, Maryland.

411 Schreiner, L.C., and J. T. Riedel, 1978. *Probable maximum precipitation estimates, United*
412 *States east of the 105th Meridian*. Hydrometeorological Report No. 51. U.S. Department of
413 Commerce: Washington D.C.

414 Stedinger, J.R., R.M. Vogel, and E. Foufoula-Georgiou, 1993. *Frequency analysis of extreme*
415 *events*, in *Handbook of Applied Hydrology*, Chapter 18, Editor, D.A. Maidment, McGraw-
416 Hill, New York.

417 Tomlinson, E.M., W.D. Kappel, G.A. Muhlestein, D.M. Hultstrand, S. Lovisone, and T.W.
418 Parzybok, 2013. Statewide Probable Maximum Precipitation Study for Ohio, Ohio Dept. of
419 Natural Resources.
420 [http://www.appliedweatherassociates.com/uploads/1/3/8/1/13810758/ohio-statewide-pmp-](http://www.appliedweatherassociates.com/uploads/1/3/8/1/13810758/ohio-statewide-pmp-final-report.pdf)
421 [final-report.pdf](http://www.appliedweatherassociates.com/uploads/1/3/8/1/13810758/ohio-statewide-pmp-final-report.pdf).

422 U.S. Army Corps of Engineers, 1973. Storm Rainfall in the United States Depth-Area Duration
 423 Data, Supplemental Sheets of Storm Studies – Pertinent Data Sheets. Department of the
 424 Army: Washington, D.C.

425 U.S. Army Corps of Engineers, 2010. Cumberland and Duck River Basins: May 2010 post flood
 426 technical report. Department of the Army: Washington, D.C.
 427 <http://cdm16021.contentdm.oclc.org/cdm/ref/collection/p266001coll1/id/2785>

428 U.S. Department of Commerce, 1951. Tables of Precipitable Water and Other Factors for a
 429 Saturated Pseudo-Adiabatic Atmosphere. U.S. Department of Commerce: Washington D.C.

430 van der Wiel, K., S.B. Kapnick, GJ van Oldenborgh, K. Whan, S. Philip, G.A. Vecchi, R.K.
 431 Singh, J. Arrighi, and H. Cullen, 2016. Rapid Attribution of the August 2016 Flood-Inducing
 432 Extreme Precipitation in South Louisiana to Climate Change. *Hydrology and Earth System
 433 Sciences* 21(2):897-921. DOI: 10.5194/hess-21-897-2017

434 van Oldenborgh G.J., K. van der Wiel, A. Sebastian, R.Singh, J. Arrighi, F. Otto, K. Haustein,
 435 S.H. Li, G. Vecchi, and H. Cullen. 2017. Attribution of Extreme Rainfall from Hurricane
 436 Harvey, August 2017. *Environmental Research Letters* 12(12):Article
 437 124009. DOI: 10.1088/1748-9326/aa9ef2

438 Wang, S.-Y. Simon, L. Zhao, and R.R. Gillies, 2016. Synoptic and Quantitative Attributions of
 439 the Extreme Precipitation Leading to the August 2016 Louisiana Flood. *Geophysical
 440 Research Letters* 43:11805-11814. DOI: 10.1002/2016GL071460

441 World Meteorological Organization, 2009. Manual for Estimation of Probable Maximum
 442 Precipitation, *Operational Hydrology Report No 1045*, WMO, Geneva, 259 pp.

443

444 **TABLE 1.** Maximum areally-averaged depths of precipitation at 1-, 3-, 6-, 12-, 18-, 24-, 36-, 48-
 445 , and 60-hour durations for areas from 1.0 km² to 129,500 km² generated from the SPAS analysis
 446 for May 1, 2010 (0100 UTC) to May 3, 2010 (1200 UTC) Nashville storm.

Maximum Average Depth of Precipitation (mm)		
May 1 (0100 UTC) – May 3 (1200 UTC) 2010		
Area	Area	Duration (hours)

(km ²)	(mi ²)	1	3	6	12	18	24	36	48	60
1.0	0.4	118	227	389	451	466	467	492	499	501
2.6	1.0	116	224	383	445	458	460	485	492	494
26	10	113	224	380	440	456	459	484	486	494
65	25	109	219	372	434	449	452	480	484	489
130	50	103	210	359	424	437	440	474	478	483
259	100	94	196	336	404	420	422	465	470	475
389	150	91	187	321	390	407	408	455	466	469
518	200	87	181	309	381	395	401	451	460	465
777	300	80	171	294	368	383	388	440	453	458
1036	400	75	164	281	358	372	379	429	448	453
1295	500	71	157	270	343	364	371	428	442	449
2590	1000	58	134	228	319	337	343	416	428	433
5180	2000	45	106	188	282	304	321	399	410	416
12950	5000	35	76	133	235	262	278	359	376	381
25900	10000	25	58	96	188	214	219	310	330	334
51800	20000	17	41	74	138	161	182	260	280	283
129500	50000	8	22	40	81	104	117	168	194	197

447

448

449 **TABLE 2.** Top five heaviest one- and two- day rainfall events at Nashville, Tennessee with
 450 estimated recurrence interval for each storm event. Period of record for this station extends from
 451 January 1940-December 2013.

Top 5	1-Day Precipitation (mm)	GEV (years)
May 1, 2010	184	792
September 13, 1979	168	308
June 4, 1998	161	205
May 6, 1984	129	35.3
March 12, 1975	120	21.2
Top 5	2-Day Precipitation (mm)	GEV (years)

May 1, 2010	345	13,833
September 13, 1979	170	33
June 4, 1998	154	18
May 6, 1984	153	17.8
March 12, 1975	152	17.0

452

453

454 **TABLE 3.** Top five heaviest one- and two- day rainfall events at Brownsville, Tennessee with
 455 estimated recurrence interval for each storm event. Period of record for this station extends from
 456 September 1895-December 2013.

Top 5	1-Day Precipitation (mm)	GEV (years)
May 1, 2010	406	929
December 25, 1987	185	38.0
January 29, 1956	170	27.1
October 6, 1910	152	17.7
March 17, 1919	152	17.7
Top 5	2-Day Precipitation (mm)	GEV (years)
May 1, 2010	457	1093
December 25, 1987	226	34.8
January 8, 1930	208	24.2
January 29, 1956	202	21.6
November 29, 2001	194	18.1

457

458

459

LIST OF FIGURES

460 **FIGURE 1.** Composite weather maps depicting surface atmospheric pressure (solid lines), areas
 461 of precipitation (shaded), and frontal positions (left column) and 500 millibar (mb)
 462 heights (solid lines), temperature (dashed lines), and wind barbs depicting wind
 463 speed and direction (right column) at 1200 UTC (0700 EST) for May 1–3 2010.
 464 Maps are adapted from the Daily Weather Map series provided by National

465 Oceanographic and Atmospheric Administration's (NOAA) Hydrometeorological
466 Prediction Center.

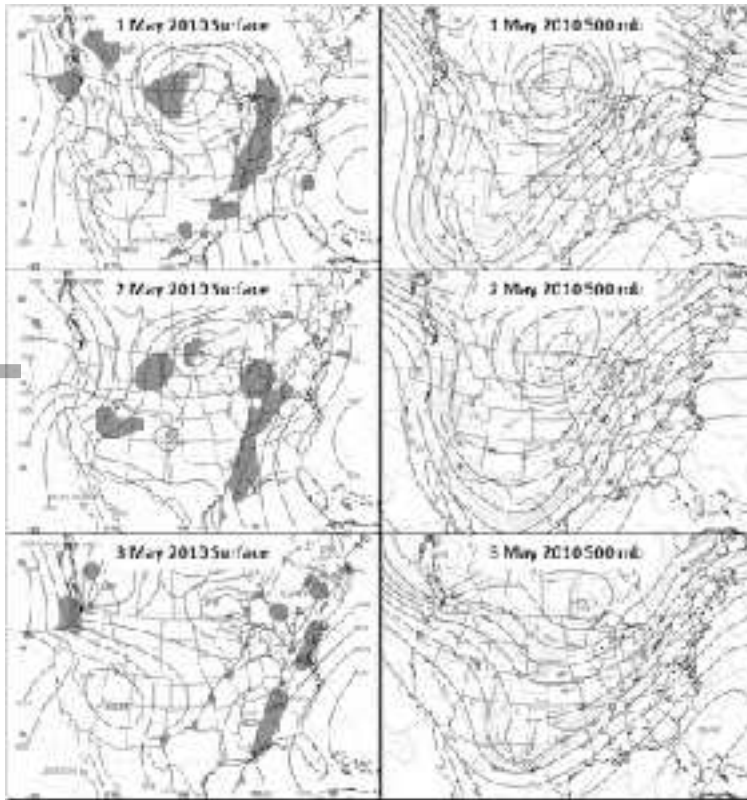
467 **FIGURE 2.** HYSPLIT backward trajectory for the May 1–3, 2010 rainfall event near Nashville,
468 Tennessee, showing the source region for the moisture-rich airmass in place during
469 the storm. Data are from the NOAA's Air Resources Laboratory.

470 **FIGURE 3.** Sixty-hour rainfall totals for May 1 (0100 UTC) to May 3 (1200 UTC) 2010 in
471 millimeters. The rainfall isohyetal pattern is generated by the Storm Precipitation
472 Analysis System (SPAS).

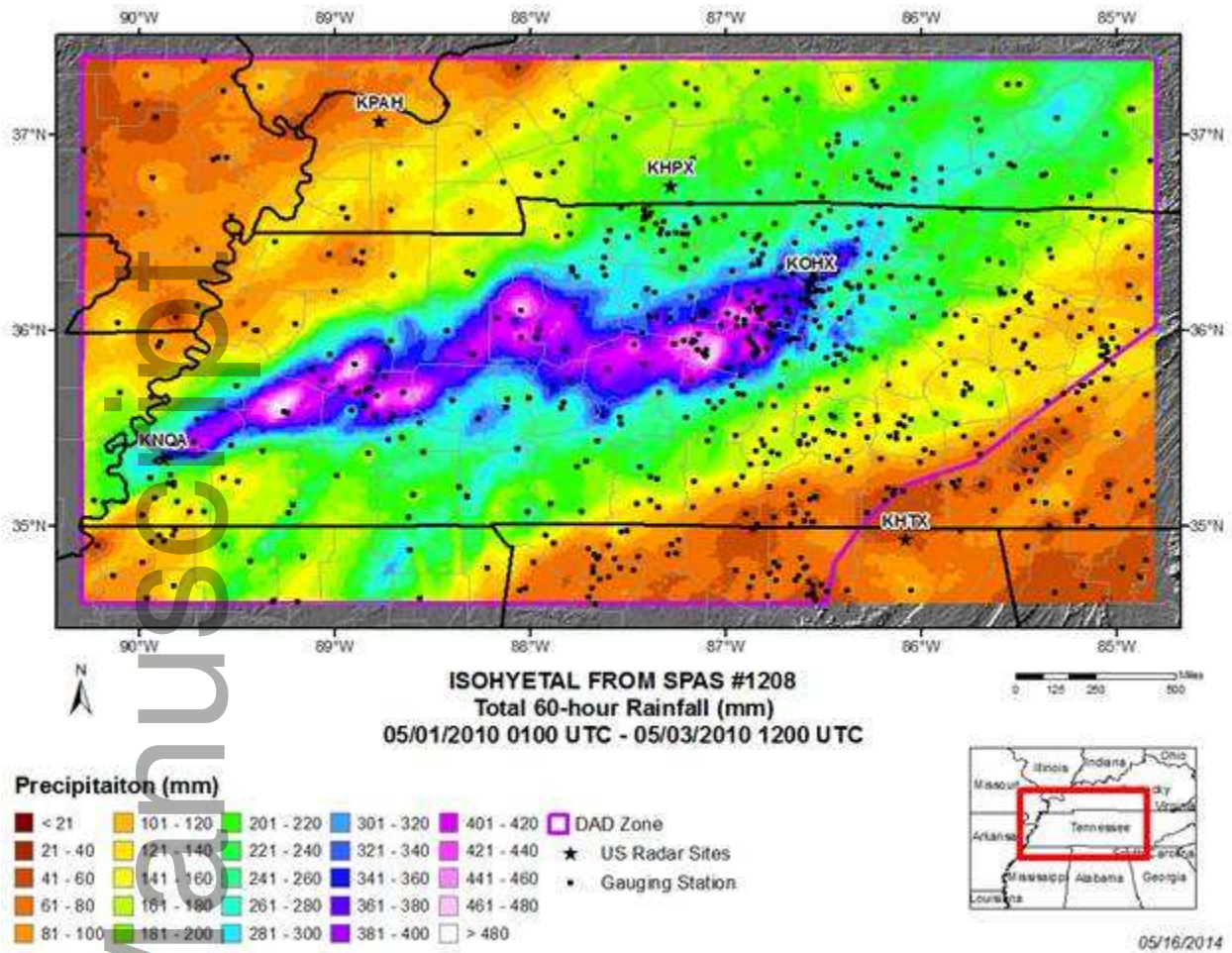
473 **FIGURE 4.** Hourly accumulations and incremental rainfall at the May 1 to 3, 2010 Nashville
474 storm center from the SPAS analysis beginning on May 1, 2010 at 0100 UTC and
475 progressing for 60 hours.

476 **FIGURE 5.** The maximum 24-hour recurrence intervals in years generated from hourly SPAS
477 rainfall values for the May 1–3, 2010 Nashville storm.

Author Manuscript

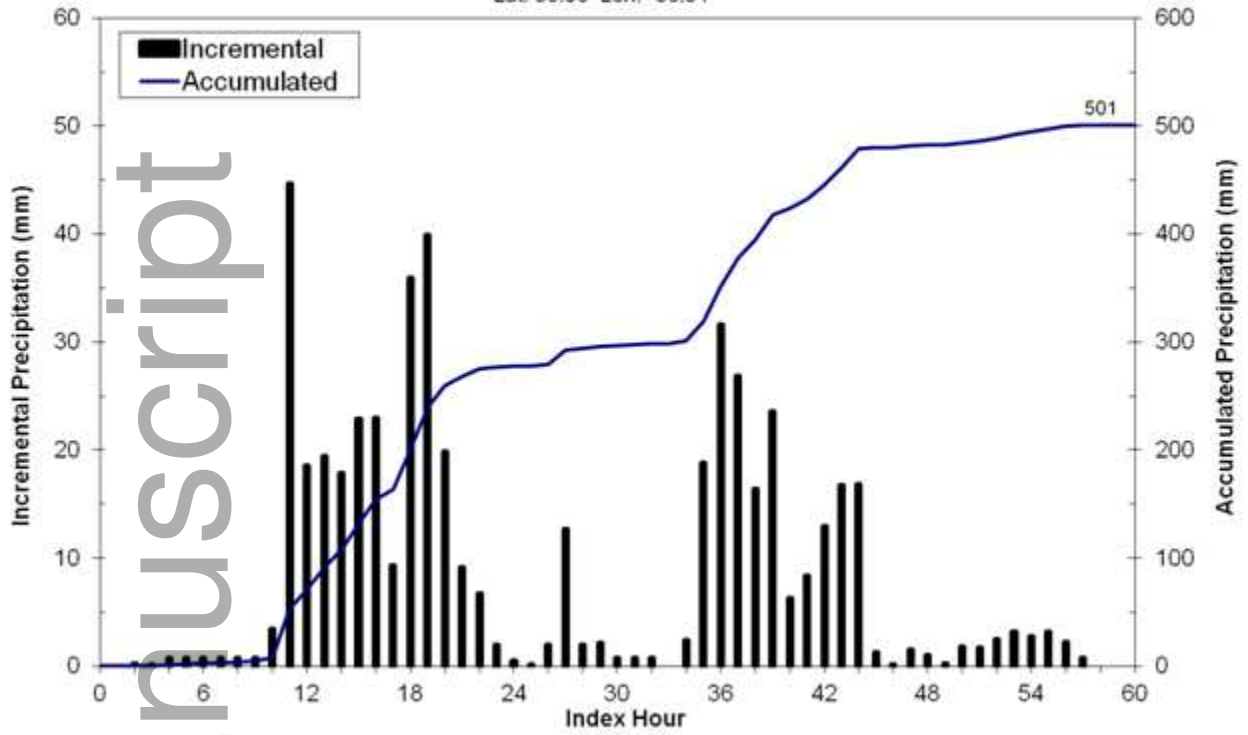


jawra_12657-17-0076_f1.tif



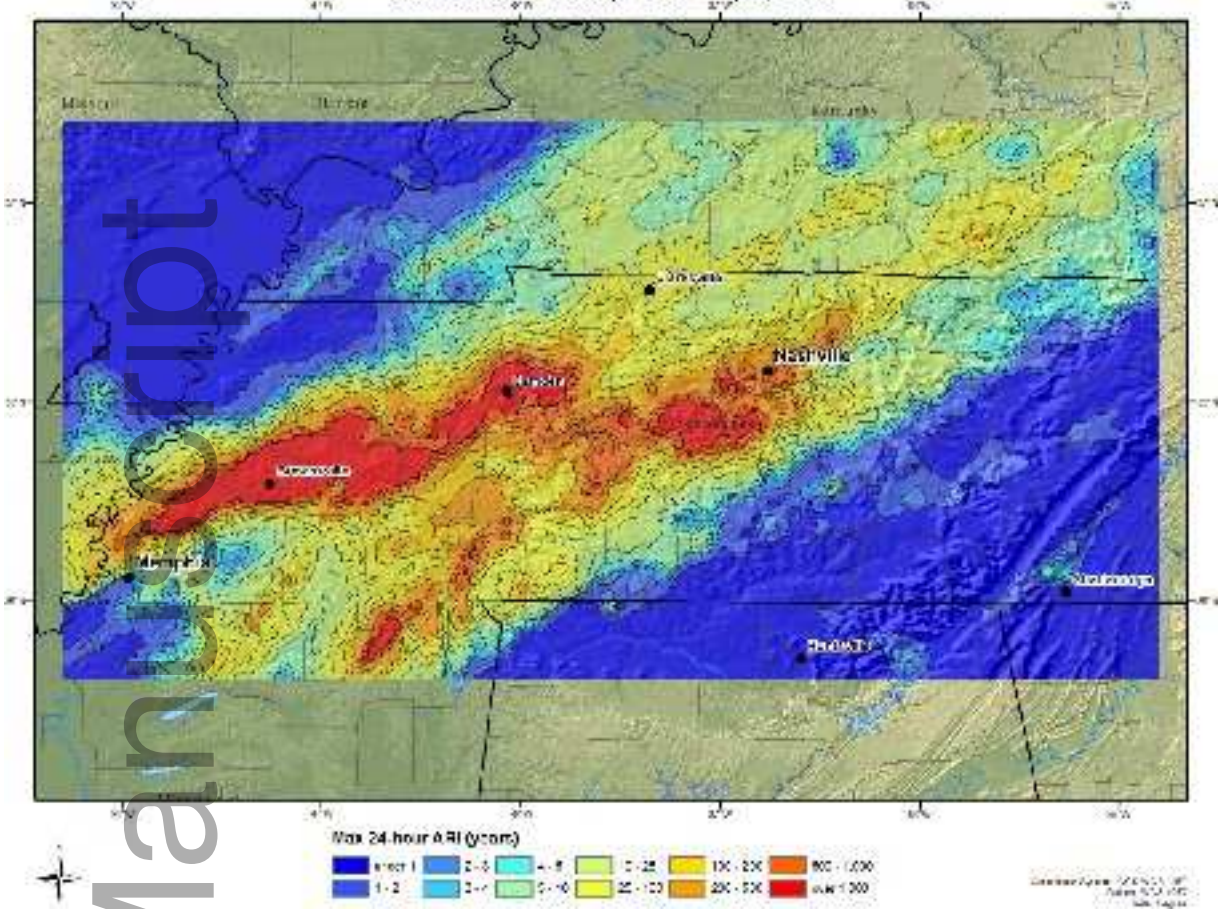
jawra_12657-17-0076_f3.tif

SPAS 1208 Storm Center Mass Curve: Zone 1
May 1 (0100 UTC) - May 3 (1200 UTC), 2010
Lat: 36.06 Lon: -86.91



jawra_12657-17-0076_f4.tif

Maximum 24-hour Average Recurrence Interval (ARI) in Years
Nashville Storm of April 30 - May 3, 2010



jawra_12657-17-0076_f5.tif